# A Novel Load Insensitive RF Power Amplifier Using a Load Mismatch Detection and Curing Technique

Donghyeon Ji, *Jooyoung Jeon and Junghyun Kim

Department of Electronics and System Engineering, Hanyang University, Ansan, 426-791, Korea
*Avago Technologies, Seoul, 137-924, Korea

***Abstract*** **— This paper proposes a new load insensitive RF power amplifier (PA) for mobile handsets using a load mismatch detection and curing technique. The PA controls a tunable output matching network (TOMN) adaptively based on the information of a mismatched load, thereby enhancing PA performances dramatically at a mismatched load without substantial performance degradation at a matched load. A load mismatch detector and TOMN can simply be implemented by using 0.18-μm silicon on insulator (SOI) FET that are integrated with 2-μm InGaP/GaAs HBT PA MMIC into a single module. To verify the idea, the PA module has been designed and implemented especially for a linearity enhancement under load mismatch condition. With WCDMA R'99 signal at 1.95 GHz, the measured results showed that ACLR at output power of 28.25 dBm was improved by as much as 13.7 dB on the worst ACLR-load angle compared to a conventional PA. In this way, the proposed load insensitive PA can keep ACLR under −37 dBc all over the load angle at 2.5:1 voltage standing wave ratio (VSWR).**

***Index Terms*** **— Antenna mismatch, SOI FET impedance mismatch detector, SOI FET TOMN, load insensitive HBT PA, linearity enhancement.**

## I. Introduction

Recently, more multifarious and stringent specifications are imposed on RF PAs in mobile devices. One of them is preserving its RF performances under antenna mismatch conditions and many efforts have been made for this purpose. Adopting an isolator between the PA and the antenna [1] and using a balanced PA [2] can be a moderate solution but these methods add the board size and they severely compromise RF performances even at a matched load. (e.g. enhance linearity at the cost of efficiency)

Alternative promising approach is to correct the mismatched impedance by using a tunable matching network (TMN) at antenna port [3]-[5]. As the method provides adaptive retuning of the TMN using a mismatch detector such that a PA load stays optimum, PA performances under antenna mismatch can be preserved. Thus, this method could be the best solution for portable devices if it can be implemented practically in view of the portability. However, since the TMN should operate under antenna mismatch (typically up to VSWR 10:1), it requires a separate extra module for accurate impedance tuning over wide antenna impedance, employing a bulky and complex TMN [3], computer-controlled control system [4], and high breakdown and high-Q MEMS switch module [5], which, however, generally has a restriction on impedance tuning range and prevents mobile devices from being miniaturized practically.

In this work, a modified 'TMN' method has been proposed integrating it to a PA module, instead of applying it to an antenna with a separate module. Thus, the impedance coverage of TMN used in this work can be much reduced due to the loss caused by post-PA components such as duplexer and switchplexer (e.g. the reduced coverage corresponds to the inner region of 2.5:1 VSWR assuming antenna mismatch as 10:1 VSWR and post-PA loss as 2.8 dB). Accordingly, the proposed technology does not need a separate tunable module and high breakdown/high-Q device for wide impedance tunability, and it can be implemented integrating a simple SOI FET detector and TOMN into a single PA module. In addition, the detector in this work was developed in a much simpler way – just detecting an impedance 'region', instead of finding a particular impedance 'value'.

To prove the idea, the proposed PA module has been developed especially for the linearity enhancement under load mismatch and has been experimentally demonstrated up to 2.5:1 VSWR conditions.

## II. Design Description

### *A. Detailed Operation of Curing System*

As can be seen in Fig. 1, a typical PA performance (e.g.

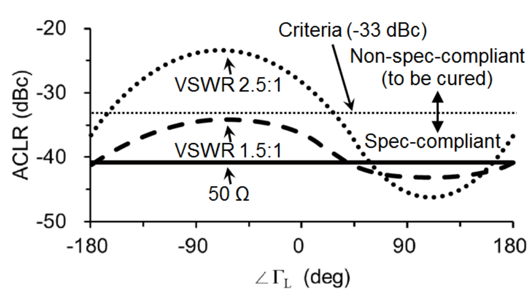


Fig. 1. Typical example of ACLR characteristic of a conventional RF PA under load mismatch condition.

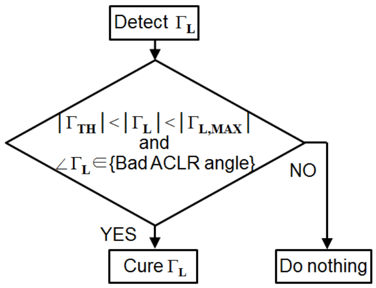


Fig. 2. Overall procedure of the proposed technique.

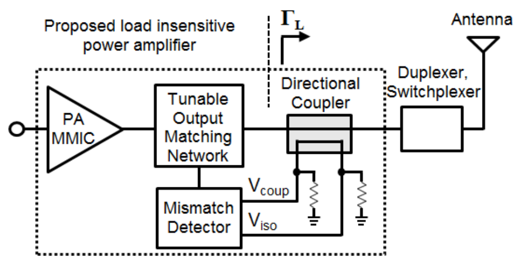


Fig. 3. Block diagram of the proposed PA module.

ACLR in Fig. 1) shows predictable trend over load impedance 'region' (instead of a 'value') represented by magnitude (or VSWR) and phase-angle ($\angle\Gamma_L$) of a load reflection coefficient ($\Gamma_L$). Thus, the spec-compliant impedance region is obviously differentiated from the other ones in a typical PA. Following strategies can lead to a good practical solution when load impedance mismatch occurs.

- On a spec-compliant region, do nothing.
- On a non-spec-compliant region, move to the spec-compliant region rather than a fixed optimum impedance value.

PA performances are typically spec-compliant when $|\Gamma_L|$ is less than a certain value referred to as $|\Gamma_{TH}|$ in Fig. 2. Even in case of larger $|\Gamma_L|$ than $|\Gamma_{TH}|$, spec-compliant region can be found in the specific $\angle\Gamma_L$ region. Thus, the region except the spec-compliant region can be specified as a non-spec-compliant region to be cured. At this moment, the higher VSWR region beyond $|\Gamma_{L,MAX}|$ ($|\Gamma_L| > |\Gamma_{L,MAX}|$) is excluded as mentioned in Sec. I. Fig. 2 shows the overall procedures of the curing system.

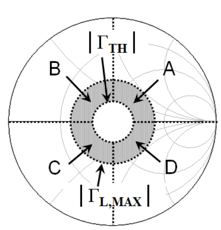


Fig. 4. Reduced and divided $\angle\Gamma_L$ regions to be considered.

Fig. 3 shows the block diagram of the proposed PA module including the mismatch detector and TOMN. The mismatch detector defines load impedance region of concerned VSWR and $\angle\Gamma_L$, and TOMN operates adaptively based on the procedure in Fig. 2. Detailed design principles of the key components are described in following subsections.

In this paper, the $\Gamma_L$ region was simply divided into four $\angle\Gamma_L$ regions (A, B, C, D in Fig. 4) and two VSWR regions by $|\Gamma_{TH}|$ (VSWR 1.5:1 in this work), and $|\Gamma_{L,MAX}|$ was assumed to be VSWR 2.5:1 as shown in Fig. 4, facilitating simultaneous detection of VSWR and $\angle\Gamma_L$ in a simple manner.

*B. Mismatch Detector*

The mismatch detector is composed of two separate circuits: one for VSWR (Fig. 5 (a)) and the other for $\angle\Gamma_L$ region (Fig. 5 (b)). Both of detectors are implemented by controlling two voltages taken at matched ports of a directional coupler ($V_{coup}$ and $V_{iso}$ in Fig. 3). $V_{iso}$ reflects the information of varying load impedance, while $V_{coup}$ is a reference voltage which is independent of the load impedance.

As for $V_{SWRD}$ in Fig. 5 (a), $V_{SWRD}$ is determined to high or low state by comparison of $V_{mag}$ and $V_{th}$, where $V_{mag}$ is from $V_{iso}$, and $V_{th}$ is from $V_{coup}$ as a design parameter to be adjusted by $V_{ctrl}$. The VSWR at the crossing point X in Fig. 6 (a) corresponds to $|\Gamma_{TH}|$ which is used as a threshold

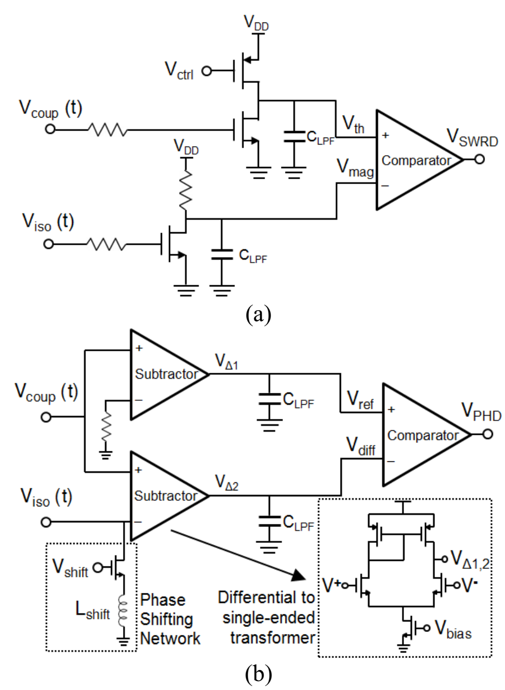


Fig. 5. Schematics of the mismatch detector: (a) VSWR detector (b) $\angle\Gamma_L$ region detector.

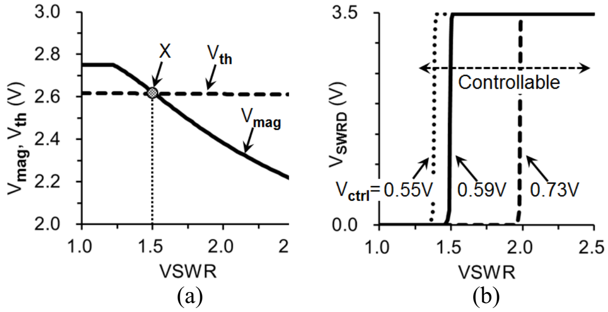


Fig. 6. VSWR detection results (sim.): (a) $V_{mag}$ and $V_{th}$ (b) $V_{SWRD}$.

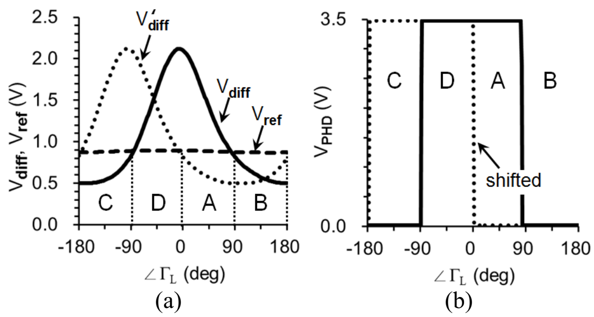


Fig. 7. $\angle\Gamma_L$ region detection results (sim.): (a) $V_{diff}$, $V'_{diff}$ and $V_{ref}$ ($V'_{diff}$: phase-shifted $V_{diff}$ ) (b) $V_{PHD}$.

for the decision of TOMN operation. The $V_{SWRD}$ is high only when $V_{mag}$ is less than $V_{th}$, which means that load VSWR can be 'in non-spec-compliant region' to be cured. In this work, $|\Gamma_{TH}|$ is VSWR 1.5:1 which is accompanied with $V_{th}$ of 2.6 V and it can be adjusted by $V_{ctrl}$ as shown in Fig. 6 (b).

The $\angle\Gamma_L$ region is detected by calculating a phase difference between $V_{coup}$ and $V_{iso}$ in Fig. 5 (b). In similar manner with $V_{SWRD}$, $V_{PHD}$ is also determined to high or low state by comparison of $V_{diff}$ and $V_{ref}$. $V_{diff}$ is a rectified voltage of the subtracted $V_{iso}$ from $V_{coup}$ and is function of $\angle\Gamma_L$. $V_{ref}$ is a reference voltage for comparing with $V_{diff}$ and is constant over $\angle\Gamma_L$ as depicted in Fig. 7 (a). Thus, $\angle\Gamma_L$ is easily divided into two regions (180° phase-duration in this work) by comparison of $V_{diff}$ and $V_{ref}$, i.e. $V_{PHD}$ in Fig. 7 (b). Furthermore, a phase shifting network (in Fig. 5 (b)) can be added at the input port of $V_{iso}$ in order to generate a phase-shifted $V_{diff}$ which is referred to as $V'_{diff}$ in dashed lines in Fig. 7 (a). In this manner, $\angle\Gamma_L$ region can be divided into four regions (90° phase-duration – A, B, C, D in Fig. 7) in a single $\angle\Gamma_L$ region detector.

### C. Tunable Matching Network

Based on the mismatch detection explained above, tunable output matching network (TOMN) operates adaptively to cure the "non-spec-compliant" region when $|\Gamma_L|$ is larger than $|\Gamma_{TH}|$. Even in this case, however, it should be noted again that there can be "spec-compliant" region ($\angle\Gamma_L$ region 'B' in this work) where TOMN provides the same impedance which is used in the case of smaller $|\Gamma_L|$ than $|\Gamma_{TH}|$. For each $\angle\Gamma_L$ region, the customized matching configuration of TOMN is applied to cure a PA performance under mismatched load. Although two switches could be enough to generate four impedance values in theory, the three switches were used for more precise curing in this work. The logic for TOMN switch control is summarized in Table I.

Table I
LOGIC TABLE FOR TOMN SWITCH CONTROL

| $\angle\Gamma_L$ region | $SW_1$ | $SW_2$ | $SW_3$ |
|---|---|---|---|
| A | OFF | | ON |
| B (spec-compliant) | OFF | ON | OFF |
| C, D | ON | OFF | |

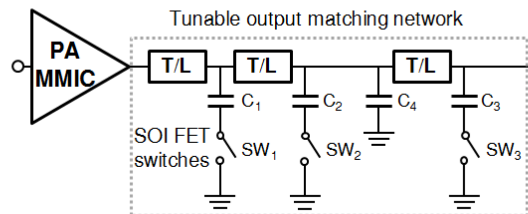


Fig. 8. Schematic of the tunable output matching network (T/L: transmission line).

## III. PA MODULE FABRICATION AND EXPERIMENTAL RESULTS

For verification purpose, a load insensitive RF PA using the proposed technique was implemented into a single module on a FR4 substrate in Fig. 9. The PA MMIC was fabricated using a 2-μm InGaP/GaAs HBT process which is designed to a 2-stage amplifier. Each emitter area of drive stage and main stage is 550, 4051 μm$^2$, respectively. The die size of PA MMIC is 800 x 650 μm$^2$. The SOI FET

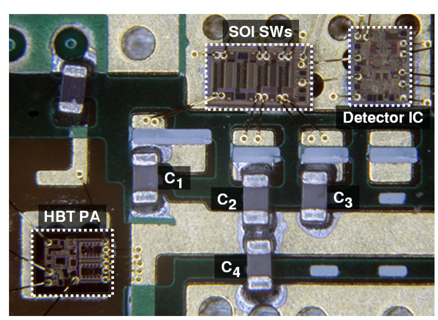


Fig. 9. Photograph of the proposed load insensitive RF PA.

TABLE II
MEASURED PERFORMANCE BEFORE AND AFTER CURING

| | **Matched (50 Ω)** | | **VSWR 2.5:1** |
|---|---|---|---|
| | PAE (%) | ACLR (dBc) | Worst ACLR (dBc) |
| Before curing | 42.9 | −40.9 | −23.4 |
| After curing (with TOMN) | 41.2 | −40.8 | −37.1 |

* Measurement condition: WCDMA R'99, 1.95 GHz, $P_{out}$=28.25 dBm and room temperature.

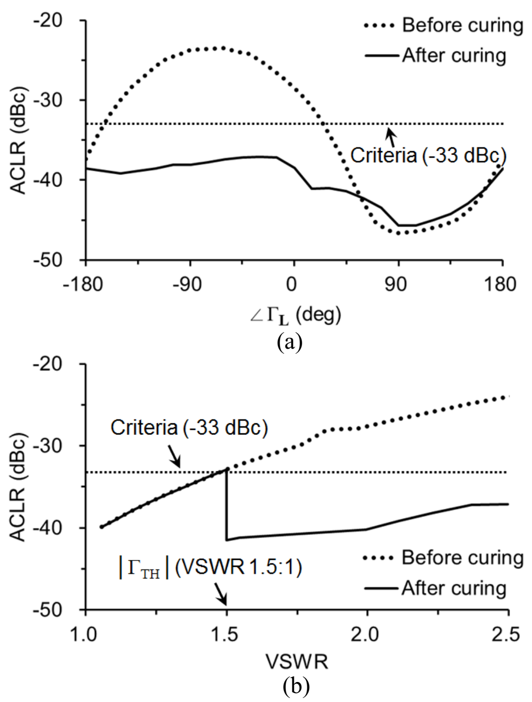


Fig. 10. Measured ACLR 28.25 dBm output power: (a) under VSWR 2.5:1 (b) at the −45° $\angle\Gamma_L$ position as the worst case.

switches and the mismatch detector were all fabricated using a 0.18-μm SOI CMOS process. The switches are designed to a stacked-FET structure. The mismatch detector is integrated in a small active size of 630 x 390 $\mu m^2$. The characterization of the curing system was performed using a commercial automated load-pull tuner with WCDMA R'99 signal centered at 1.95 GHz under room temperature and linear power of 28.25 dBm.

The measurement of PA basic performance was summarized in Table II. The ACLR was dramatically improved by 13.7 dB after curing at the worst $\angle\Gamma_L$ position of VSWR 2.5:1, accompanying PAE degradation of 1.7% due to TOMN loss but maintaining ACLR at well matched condition (50 Ω). Fig. 10 shows the improved results after curing ACLR per $\angle\Gamma_L$ at VSWR 2.5:1 (Fig. 10 (a)) and per VSWR at the worst $\angle\Gamma_L$ (Fig. 10 (b)), respectively, when compared to before curing. The ACLR was maintained below the specification of −37 dBc for the entire range of load variations, thus verifying the effectiveness of the proposed load mismatch detection and curing technique for RF PA application.

## IV. CONCLUSION

A novel load insensitive PA for mobile handsets has been presented to provide a practical solution for linearity degradation caused by antenna mismatch. By applying a TMN to the PA output, the curing system can be configured in a simple form and the linearity degradation under antenna mismatch condition has been cured more easily. The evaluated PA achieved 13.7 dB linearity improvements at full- under the worst antenna mismatch condition just at the cost of 1.7% efficiency degradation at a matched load.

In spite of not being presented in this work, other PA performances such as efficiency and total radiated power (TRP) can also be cured in this manner. Furthermore, this method can be easily extended to the 4th-generation (4G) LTE PA development. Besides, the "non-spec-compliant" impedance region can be subdivided into more than four $\angle\Gamma_L$ regions in case that more precise mismatch detection is needed.

## ACKNOWLEDGEMENT

This work was supported by the Basic Science Research Program through the National Research Foundation of Korea (NRF) funded by the Ministry of Education, Science and Technology (2012-0001888).

## REFERENCES


[1] A. van Bezooijen, C. Chanlo, and A.H.M van Roermund, "Adaptively preserving power amplifier linearity under antenna mismatch," *IEEE MTT-S Int. Microwave Symp. Dig.*, Vol. 3, pp.1515-1518, June 2004.

[2] G. Berretta, D. Cristaudo, and S. Scaccianoce, "A balanced cdma2000 SiGe HBT load insensitive power amplifier," *IEEE Radio and Wireless Symp*., pp. 523- 526, January 2006.

[3] D. Qiao, D. Choi, Y. Zhao, D. Kelly, T. Hung, D. Kimball, M. Li, and P. Asbeck, "Antenna impedance mismatch measurement and correction for adaptive CDMA transceivers," *IEEE MTT-S Int. Microwave Symp. Dig*., pp.783-786, June 2005.

[4] A. Keerti, and A. Pham, "Dynamic output phase to adaptively improve the linearity of power amplifier under antenna mismatch," *IEEE RFIC Symp. Dig*., pp.675-678, June 2005.

[5] A. van Bezooijen, M. A. de Jongh, C. Chanlo, L. C. H. Ruijs, F. van Straten, R. Mahmoudi and A. H. M. van Roermund, "A GSM/EDGE/WCDMA Adaptive Series-LC Matching Network Using RF-MEMS Switches," *IEEE journal of Solid-State Circuits*, vol. 43, no. 10, pp. 2259-2268, October 2008.